Mon. Not. R. Astron. Soc. **000**, 000–000 (0000) Printed 4 December 2007 (MN LATEX style file v1.4)

The separation of the stars in the binary nucleus of the planetary nebula Abell 35

A. A. Gatti[1], J. E. Drew[1], R. D. Oudmaijer[1], T. R. Marsh[2], A. E. Lynas-Gray[3]

[1] *Imperial College of Science, Technology and Medicine, Blackett Laboratory, Prince Consort Road, London, SW7 2BZ, U.K.*
[2] *Department of Physics, Southampton University, Southampton S09 5NH, U.K.*
[3] *Department of Physics, University of Oxford, Nuclear Physics Laboratory, Keble Road, Oxford, OX1 3RH, U.K.*

received, accepted

ABSTRACT

Using the Planetary Camera on board the Hubble Space Telescope we have measured the projected separation of the binary components in the nucleus of the planetary nebula Abell 35 to be larger than 0.08″ but less than 0.14″. The system was imaged in three filters centered at 2950Å, 3350Å and 5785Å. The white dwarf primary star responsible for ionizing the nebula is half as bright as its companion in the 2950Å filter causing the source to be visibly elongated. The 3350Å setting, on the other hand, shows no elongation as a result of the more extreme flux ratio. The F300W data allows the determinination of the binary's projected separation. At the minimum distance of 160 parsec to the system, our result corresponds to 18±5 AU. This outcome is consistent with the wind accretion induced rapid rotation hypothesis, but cannot be reconciled with the binary having emerged from a common-envelope phase.

Key words: ISM: planetary nebulae: individual (Abell 35) binaries: close binaries: general stars: evolution stars: peculiar

1 INTRODUCTION

The planetary nebula Abell 35 (α_{50}=$12^h50.9^m$, δ_{50}=$-22^o36'$; l=303^o, b=$+40^o$) was hypothesized to possess a binary nucleus by Jacoby (1981) to account for the apparent lack of an ionizing source and for the blue excess of LW Hya (BD -22°3467), the bright G8 III-IV star, visible off-center within the nebula. The white dwarf primary was first reported in IUE SWP spectra taken by Grewing and Bianchi (1988).

Because of a number of extraordinary features, Abell 35 has represented a challenge to theories of binary star evolution. More specifically:

(i) The optically-dominant cool component, LW Hya, is distinguished from normal G stars by its remarkably high projected rotational velocity (vsin i=90 km s^{-1}, Vilhu, Gustaffson & Walter, 1991). G type stars with such large vsin i are rare and usually classified as FK Comae objects. The origin of FK Comae stars is unclear, although it has been suggested that they are either coalesced/coalescing contact binaries (e.g. see Welty & Ramsey, 1994) or the remnants of a mass transfer event with a thus far undetected white dwarf companion (Walter & Basri, 1982).

(ii) Long-term radial velocity measurements of BD -22°3467 have shown no evidence of variations due to orbital motion (Gatti et al., 1997), suggesting that an orbital period in excess of 10 years could well turn out to be appropriate.

(iii) Based on their low-dispersion UV spectrum, Grewing and Bianchi (1988) noted that the white dwarf central star bears close resemblance to the class of PG 1159 objects (Werner et al. 1996). These are rapidly pulsating hot stars which have just joined or are about to join the white dwarf cooling track.

LoTr 1 and LoTr 5 (Longmore & Tritton, 1980) are the only other planetary nebulae believed to have similar central star binaries to that in Abell 35. The three systems are therefore often referred to as the Abell 35-like objects.

Two evolutionary scenarios have been invoked to explain the Abell-35 like nuclei. The first of these is the "common envelope" hypothesis (Bond and Livio, 1990) according to which the binary's primary has undergone dynamically unstable Roche Lobe overflow. The second, the "wind accretion induced rapid rotation" model where slow accretion of the AGB wind from the white dwarf progenitor in a detached configuration accounts for the angular momentum transfer that spins up the companion (eg. Jeffries & Stevens, 1996 and references therein). Since the common envelope scenario involves the primary star expanding to fill its Roche Lobe, while the wind accretion model applies to a fully-detached

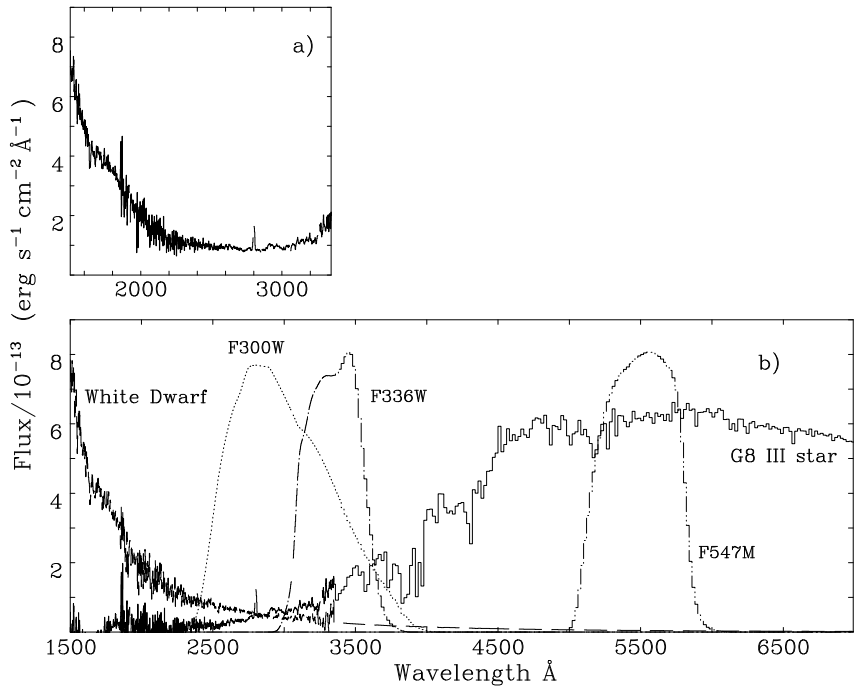

Figure 1. a) the SWP and LWP IUE spectrum of the central star of Abell 35. b) The IUE spectrum decomposed into its white dwarf and G star contributions (see text for details). Also shown are the relevant WFPC2 filter profile functions. The relative flux contributions of the two components in the different filters were calculated by folding the filter profiles with the single-star spectra and comparing.

Table 1. Log of exposures. Sub-pixel offsets were applied for "drizzling" purposes to both the F300W and the F336W filters.

Filter	Exp. time	HJD
F300W	60.0s	2450824.107
F300W	60.0s	2450824.110
F300W	60.0s	2450824.112
F300W	60.0s	2450824.115
F336W	12.0s	2450824.121
F336W	12.0s	2450824.123
F336W	12.0s	2450824.125
F336W	12.0s	2450824.127
F547M	0.4s	2450824.131
F547M	0.4s	2450824.133
F547M	0.4s	2450824.135
F547M	1.0s	2450824.136
F547M	1.0s	2450824.137

configuration, a distinction between these models may arise from a clear determination of the present-day binary separation.

As part of a wider programme of observation of the nucleus of Abell 35, we have obtained HST Planetary Camera (PC) images of it spanning the UV and optical domain, with a view to finding out if the binary is spatially resolvable. If it is, we can establish a lower limit on the radius of the binary orbit which may rule out the common envelope hypothesis. The pixel size of the PC is 45.5 mas which corresponds to a projected separation of 8 AU at 160 pc, the likely minimum distance to Abell 35 (see section 4). Prior to this work, the separation was only constrained to be below ~ 1 arcsec from IUE data. We will now present HST PC data which shows the binary to be resolvable.

2 OBSERVATIONS

In January 1998, the Hubble Space Telescope Wide Field PC 2 was used to obtain 13 exposures (Table 1) of the binary nucleus of Abell 35 in three filter settings: F300W ($\lambda_c \sim 2950$Å, $\lambda\lambda \sim$ 2300–4000 Å), F336W ($\lambda_c \sim 3350$Å, $\lambda\lambda \sim$ 2900–3800 Å) and F547M ($\lambda_c \sim 5785$Å, $\lambda\lambda \sim$ 5000 – 6000 Å). Based on the IUE SWP and LWP spectra of the system (Grewing and Bianchi, 1988; Jasniewicz et al. 1994), the G8 III-IV star starts to dominate the total flux longwards of 2800 Å. To determine quantitatively the relative flux of the two stellar components in each filter, the IUE spectra were decomposed for its white dwarf and G-star contributions by comparison with a PG1159-type white dwarf IUE spectrum (fig 1). The result was then extrapolated to higher wavelengths assuming a Rayleigh-Jeans wavelength dependence for the white dwarf and using either a 5000K or a 5500K, log g=3.5, Kurucz model atmosphere normalized to V=9.6mag for the G-star. The resulting single-star spectra for both components were then folded with the WFPC2 filter profile functions. Depending on whether a temperature of 5000 or 5500K is assumed for the G star, we find the expected G star to white dwarf flux ratio to be: 1.8–2.2 for the F300W filter, 5.3–6.2 for the F336W filter and 115–122 for the F547M filter.

Both the F300W and F336W exposures were sub-

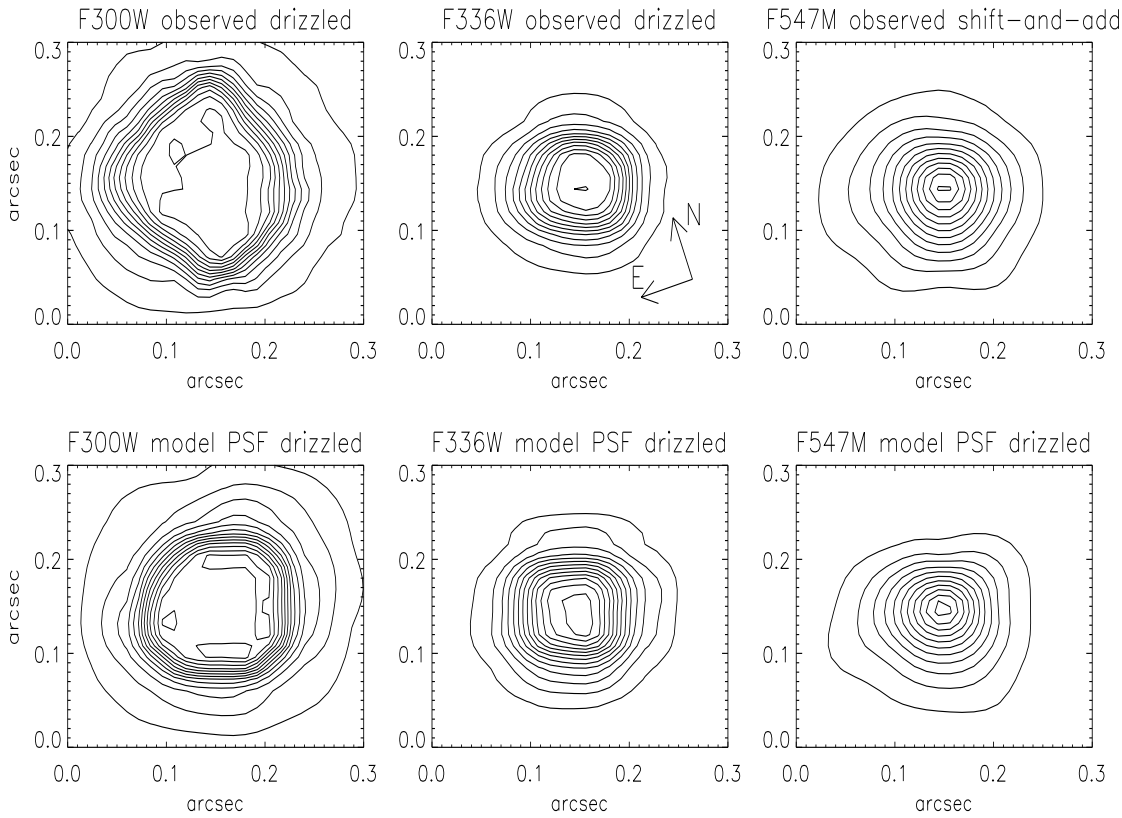

Figure 2. The observed images (top) and the TINYTIM produced model point spread functions (bottom) for all three filters: F300W, F336W and F547M. The F300W and F336W have been "drizzled" to a pixel size of 22.75 mas, half the original PC size. The F547M images, on the other hand, retain the original PC size. The F300W model image has been saturated to the known level. The observed F300W image is clearly elongated with respect to the PSF along a ∼NNE–SSW axis that is almost perpendicular to a slight elongation apparent in the PSF itself. The contour levels indicate 6% flux steps.

stepped by a non-integral pixel amount to allow the recovery of high frequency spatial information lost by the factor of two undersampling of the PSF by the pixels of the PC. These multiple offset images were linearly reconstructed using the DRIZZLE software written by Fruchter & Hook (1996). The validity of the reconstructed, higher resolution, images was assessed in both filters by comparison with a reconstruction performed without change in pixel size (i.e. by using the DRIZZLE routine to simulate a straightforward shift-and-add procedure). The F547M exposures were simply co-added after correcting for cosmic rays. In all cases the root-mean-square jitter of the telescope was found to be ≤ 7.0 mas, indicating no large excursions of the tracking during the individual exposures.

Further, for each filter, model point spread functions to be compared with the data were generated with the TINYTIM software (Krist, 1995). A number of subsampling parameters were used and, when necessary, the resulting models were rescaled and convolved with the pixel response kernel.

3 RESULTS

The leftmost two panels of figure 2 show the F300W drizzled image and the PSF as modelled by TINYTIM for a G8 spectral type object (which does not differ noticeably from the PSF appropriate to a hot white dwarf). It can be seen immediately that there is an elongation of the observations in an approximately NS direction which cannot be directly related to an artifact of the PSF. However, because the F300W image is saturated (due to A/D conversion only, and not to blooming), it is necessary to assess whether the elongation could have been induced by an optical error in the F300W filter made more acute by effect of the saturation. We have done this by producing artificial images for a number of source separations and position angles. To compare with the data we have scaled the relative counts of the two components to the flux ratio calculated from the IUE spectra and saturated the images to the known level. We have then drizzled the images following the same procedure as with the observations.

A meaningful comparison of the simulated data with the observations is not trivial. Mainly as a result of pixellation effects and because of the intrinsic asymmetry of the WFPC2 PSFs, the overall shape of the calculated image and its resulting center change subtly as a function of the position angle of the two sources. A χ^2 minimization procedure cannot be used as a similarity test because of its strong dependence on an accurate alignment between models and observations. The overall shape of the model images, on the other hand, can. We have quantified this by measuring the

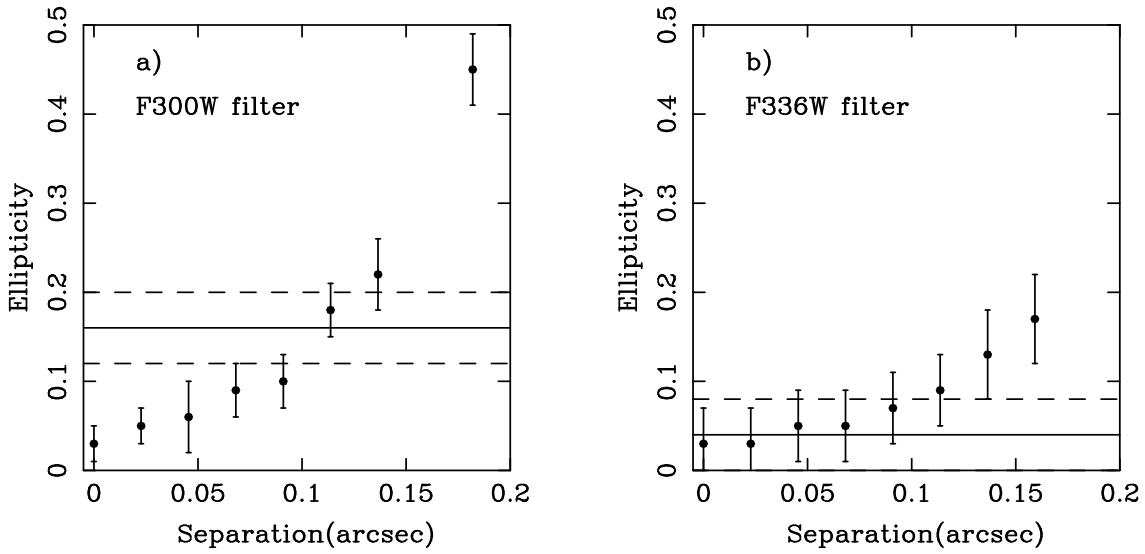

Figure 3. a) The ellipticity as a function of separation for F300W model images produced with TINYTIM. Each value is the average ellipticity for 8 models with fixed separation and varying position angles encompassing all 360° in 45° steps. The 3σ error bars reflect the uncertainty in the measured ellipticity as a function of position angle mainly due to pixellation effects. The solid line is the measured ellipticity of the observed F300W image with the associated error. Only separations in the range 0.08-0.14 arcsec are consistent with the observations. Smaller separations cannot account for the elongation of the F300W data. The non zero ellipticity of a single source point spread function reflects its slight elongation in a direction almost perpendicular to the observation (fig 2). Panel b) shows the result of the analysis applied to the F336W images. In this circumstance, the observations are consistent with a binary source with orbital separation $\leq 0.14''$, consistent with the upper limit produced by the F300W data.

image ellipticity as a function of separation for the models and comparing this with the F300W observations (fig 3a). Ellipticity measurements are independent of the image centers but vary slightly with assumed position angle (again mostly due to pixellation effects). Models spanning position angles 0-315 in steps of 45 degrees were made and the average ellipticity was calculated. The error bars shown in fig 3 are 3σ, and were determined from the ellipse fitting routine. They also reflect the scatter with changing position angle. The ellipticity of the F300W data was found to be 0.16±0.04, inconsistent with the data arising from a single, unresolved, point source with a plausible PSF. In fact, only separations in the range 0.08-0.14 arcseconds can be reconciled with the observed F300W image. In view of the 3σ significance of the error bars used here, this must be regarded as a maximum allowable range.

This result was further checked against the F336W data. The lack of any detectable elongation in this filter (fig 2, middle panels) is not surprising in view of the more extreme flux ratio and modest separation of the sources, suggested by the F300W data. We have modelled the F336W data following the same procedure as for the F300W observations, varying the separation and adopting a flux ratio of 5 (which maximizes the white dwarf flux contribution). This ellipticity test reveals the F336W filter to be far less sensitive to the binary separation. In fact, we find that no significant elongation appears in the overall F336W image until a separation of the order of 0.12–0.14 arcsecs is reached (fig 3b). The F336W observation therefore sets the same upper limit of 0.14 arcseconds on the separation of the binary components as the F300W data.

Hence, on the basis of the F300W data, we conclude that the projected separation of the binary components falls in the range 0.08–0.14 arcseconds.

Table 2. Estimates of the distance to Abell 35

D(pc) (ref)	method	comments
240 (1)	H_α + [NII] line flux	—
208 (2)	5 GHz radio flux	—
360 ± 80 (3)	photometry	—
~ 310 (4)	blackbody fit to WD	$M_{WD} = 0.6 M_\odot$
134^{+33}_{-23} (5)	Trigonom. Parallax	uncorrected for bias

[1]Abell, 1966;[2] Milne, 1979;[3]Jacoby, 1981;[4]Hollis et al., 1996; [5] ESA, 1997

4 DISCUSSION AND CONCLUSION

The translation of the derived separation of into a projected orbital separation requires a reliable distance to Abell 35. This is not yet available. In table 2 we present a short summary of the distance estimates to Abell 35 currently in the literature.

The recent Hipparcos measurement ($\pi = 7.48 \pm 1.55$ mas) seems to suggest a substantial decrease in the distance compared to previous estimates. However, the value in table 2 should be corrected for the Lutz-Kelker statistical bias which leads to an under-estimate of the distance to an object (Lutz & Kelker 1973; Koen 1992; see also Oudmaijer, Groenewegen & Schrijver 1998). Koen (1992) calculated the bias

analytically and provided 90% confidence intervals of the bias. Although the relative error of $\sim 20\%$ in the observed parallax for LW Hya is just too large to be calculated analytically, we may gain some insight by applying the bias correction for a 17.5% error (Koen's maximum value) to the data of Abell 35. This leads to a (mean) bias corrected distance of 163^{+96}_{-58} pc. In view of the earlier distance estimates, we adopt 160 pc as a *minimum* distance.

At 160 pc, the measured separation between the white dwarf and the G-star translates into a *projected* orbital separation of 18±5 AU. For this minimum value of the orbital separation, and a likely maximum total mass of the system of $\sim 3M_\odot$ we find that the orbital period for a circular orbit about the system's barycenter is P > 40 years. This estimate is consistent with Gatti et al.'s (1997) conclusion that the binary period must be longer than 10 years. Should the orbit turn out to be significantly eccentric, our minimum period estimate would not apply.

The results presented in this paper exclude the possibility that Abell 35 may be the remnant of a common-envelope phase. For example, if we assume a relatively favourable initial configuration of a $5M_\odot$ AGB primary and a $1M_\odot$ secondary at the minimum acceptable orbital separation of 13 AU (obtained for the minimum distance of 160 pc and minimum projected separation of 0.08 arcsec), we can estimate the Roche Lobe radius of the primary to be ∼7 AU (Eggleton, 1983). This figure is itself a minimum given that the common-envelope phase is expected to result in orbit shrinkage. Since no AGB star can reach a 7 AU radius without breaking the core mass-luminosity relation (Paczynski, 1970), the primary star in Abell 35 cannot have filled its Roche Lobe.

On the other hand, by inspection of the model results presented by Jeffries & Stevens (1996) we find that, at separations matching or exceeding the minimum deduced from our data, the spin up of the companion star BD -22°3467 to a period of 18 hours (Jasniewicz & Acker, 1988) is easily achieved by accreting a few percent of a solar mass. This is entirely consistent with values for wind accretion rates obtained in hydrodynamical models of binary stars (Theuns, Boffin & Jorissen 1996 and references therein). Important tasks for the future are to test wind-accretion models more precisely by, for example, obtaining constraints on the present-day component masses in this intriguing binary.

ACKNOWLEDGMENTS

The authors are extremely grateful to Jeremy Walsh and Richard Hook for their help in the analysis of the WFPC2 images. We would also like to thank the referee, George Jacoby, for his useful comments. AAG acknowledges financial support from the Knight Award of the University of London, from the Department of Physics of Imperial College and from the University of Rome 'La Sapienza'. This work is based on observations with the NASA/ESA Hubble Space Telescope obtained at the Space Telescope Science Institute, which is operated by AURA Inc. under contract to NASA.

REFERENCES

Abell G. O., 1966, ApJ, 144, 259
Bond H. E., Livio M., 1990, ApJ, 355, 568
Eggleton P. P., 1983, ApJ, 268,368
ESA, 1997, The Hipparcos and Tycho Catalogues, ESA SP-1200
Fruchter A., R. Hook, 1996, Applications of Digital Image Processing XX, ed. A. Tescher, Proc. S.P.I.E. vol 3164
Gatti A. A., Drew J. E., Lumsden S., Marsh T., Moran C., Stetson P., 1997, MNRAS, 291, 773
Grewing M., Bianchi L., 1988, in *A Decade of UV Astronomy with IUE*, ESA SP-281, 2, 177
Hollis J. M., Van Buren D., Vogel S. N., Feibelman W. A., Jacoby G. H., Pedelty J. A., 1996, ApJ, 456, 644
Jacoby G. H., 1981, ApJ, 244, 903
Jasniewicz G., Acker A., 1988, A&A, 189, L7
Jasniewicz G., Lapierre G., Monier R. 1994, A&A, 287, 591
Jeffries R. D., Stevens I. R., 1996, MNRAS, 279, 180
Koen, C., 1992, MNRAS, 256, 65
Krist J., 1995, in *Astronomical Data Analysis Software and Systems IV*, eds. Shaw R. A., Payne H. E., Hayes J. J. E., ASP Conf.Ser.No. 77, 349
Longmore A. J., Tritton S. B., 1980, MNRAS, 193, 521
Lutz T. E., Kelker D. H., 1973, PASP, 85, 573
Milne D. K., 1979, A&AS, 36, 227
Oudmaijer R. D., Groenewegen M. A. T., Schrijver H., 1998, MNRAS, 294, L41
Paczynski B., 1970, Acta Astron. 20, 47
Theuns T., Boffin H. M. J., Jorissen A., MNRAS, 280, 1264
Vilhu O., Gustafsson B., Walter F. M., 1991, A&A, 241,167
Walter F. M., Basri G. S., 1982, ApJ, 260, 735
Welty A. D., Ramsey L. W., 1994, ApJ, 435, 848
Werner K., Dreizler S., Heber U., Rauch T., 1996, in *Hydrogen Deficient Stars*, eds. Jeffery C. S., Heber U., ASP Conf.Ser.No. 96, 267